Interdisciplinary Research in Medical Sciences Specialty
ISSN: 3062-4401
2025, Volume 5, Issue 2, Page No: 131-149

Available online at: www.galaxypub.co/page/journals

Galaxy Publication

CRISPR-Cas9 Screening and Multi-Omics Reveal the CHD7–ANGPT1 Axis as a Driver of Multidrug Resistance in Acute Myeloid Leukemia

Emma Wilson[1]*, Frederik De Jong[2], Lara Peters[2]

[1]Department of Hematology and Drug Resistance Research, Faculty of Medicine, University of Edinburgh, Edinburgh, United Kingdom.
[2]Department of CRISPR Screening and Multi-Omics Integration, Faculty of Pharmaceutical Sciences, Utrecht University, Utrecht, Netherlands.

***E-mail** ✉ emma.wilson@ed.ac.uk

Received: 02 June 2025; **Revised:** 04 August 2025; **Accepted:** 10 August 2025

ABSTRACT

Acute myeloid leukemia (AML) is an aggressive hematological cancer and ranks among the most frequent leukemias observed in adults. Although new targeted treatments have recently been developed and approved, the emergence of drug resistance continues to present a serious therapeutic barrier. This investigation utilized an unbiased CRISPR-Cas9 gene knockout screen in AML cell lines to discover unrecognized factors contributing to resistance against the approved FLT3 inhibitor gilteritinib. The screen pinpointed chromodomain helicase DNA binding protein 7 (CHD7) as a previously unidentified modulator of therapeutic resistance. Notably, inactivation of CHD7 not only produced resistance to FLT3-targeted agents but also generated cross-resistance to a wide array of drugs, such as venetoclax and daunorubicin (DNR). Integrated transcriptomic and proteomic analyses indicated that deletion of CHD7 elevates angiopoietin-1 (ANGPT1) levels, which promotes resistance by stimulating the PI3K/AKT and MAPK/ERK pathways. Importantly, reducing ANGPT1 expression through genetic knockdown or blocking its receptor TIE2 with pharmacological agents partially reversed drug insensitivity in cells lacking CHD7. Overall, these results highlight the CHD7-ANGPT1 signaling axis as a novel contributor to multidrug resistance in AML. Preclinical evidence additionally supports the potential of combining targeted AML therapies with TIE2 inhibitors as an effective means to counteract drug resistance.

Keywords: Acute myeloid leukemia, ANGPT1, CHD7, Drug resistance, Gilteritinib, Multi-omics

How to Cite This Article: Wilson E, De Jong F, Peters L. CRISPR-Cas9 Screening and Multi-Omics Reveal the CHD7–ANGPT1 Axis as a Driver of Multidrug Resistance in Acute Myeloid Leukemia. Interdiscip Res Med Sci Spec. 2025;5(2):131-49. https://doi.org/10.51847/ck7MScPl6m

Introduction

Acute myeloid leukemia (AML) constitutes a biologically heterogeneous hematological malignancy marked by aberrant expansion of myeloid progenitors [1, 2]. It represents the predominant subtype of acute leukemia in adults, typically diagnosed at a median age of 68 years [3]. Older individuals commonly experience reduced tolerance to treatment and face a particularly dismal outlook [4]. Although conventional chemotherapy combined with stem cell transplantation achieves success in certain cases, long-term cure rates are limited to 35–40% overall and decline to less than 15% among elderly patients [5]. The therapeutic paradigm for AML has shifted considerably in recent years, moving away from intensive cytarabine- and anthracycline-containing “3 + 7” protocols toward precision-targeted agents and immunotherapeutic approaches, yielding clear advances in patient outcomes [6].

Substantial research conducted over the last two decades has uncovered multiple recurrent driver mutations in AML, notably those involving FLT3, NPM1, and DNMT3A. FLT3 mutations are among the most frequent, affecting roughly 30% of cases [7]. These alterations disrupt transcriptional and epigenetic regulation, fuel uncontrolled proliferation of leukemic cells, and bolster survival signals via persistent stimulation of pathways

such as PI3K/AKT, MAPK/ERK, and JAK/STAT, all of which are linked to inferior clinical results [8-10]. Consequently, several targeted drugs have gained clinical approval, including FLT3 inhibitors (gilteritinib, midostaurin, quizartinib) [11], the BCL-2 inhibitor venetoclax [12], IDH inhibitors (enasidenib, ivosidenib), and PD-L1 inhibitors such as atezolizumab. These agents have contributed to meaningful improvements in clinical responses for AML patients [13].

Despite these developments, drug resistance and short-lived remissions remain critical limitations [14-17]. Emerging evidence has illuminated varied molecular processes responsible for resistance to FLT3 inhibitors and venetoclax. Resistance against FLT3 inhibitors commonly develops through secondary mutations in FLT3 itself, engagement of compensatory signaling routes (for example, RAS/MAPK), and supportive interactions within the bone marrow niche that protect leukemic cells [18- 20]. Venetoclax resistance, conversely, frequently involves overexpression of other anti-apoptotic members of the BCL-2 family (such as MCL-1 and BCL-XL), alterations in cellular metabolism and mitochondrial function, and reactivation of survival pathways including PI3K/AKT and MAPK/ERK [21-23]. Such findings illustrate the multifaceted and interconnected nature of resistance mechanisms in AML, highlighting the urgent need for deeper mechanistic understanding to support rational combination therapies.

CHD7 is an ATP-dependent chromatin remodeler known to regulate hematopoietic stem and progenitor cell populations through functional cooperation with RUNX1, a central transcription factor governing endothelial-to-hematopoietic transition in early development [24-27]. In oncology, CHD7 loss has been shown to delay CBFB-MYH11-associated leukemia development in murine models [28]. CHD7 also influences the AK4-AMPK-p53 pathway, thereby enhancing proliferation of colorectal cancer cells in both culture and animal systems [29]. Dysregulated CHD7 levels have furthermore been associated with tumor-promoting activities across multiple cancer types and with poorer patient prognosis [30, 31]. Nevertheless, its potential contribution to drug resistance has scarcely been investigated.

A comprehensive understanding of the pathways driving drug resistance in AML is vital for elucidating leukemogenic signaling networks and for creating effective strategies to restore treatment sensitivity [32]. The current work employed a CRISPR-Cas9-based genome-wide knockout screen in AML cells, which identified CHD7 as a novel gene whose absence induces resistance to several clinically relevant agents, including gilteritinib and venetoclax. Follow-up multi-omics profiling established that CHD7 loss elevates ANGPT1 expression, thereby activating the PI3K/AKT and MAPK/ERK cascades to drive broad drug resistance. In addition, preclinical evaluation suggests that pairing targeted therapies with inhibitors of TIE2—the receptor for ANGPT1—may provide a valuable therapeutic avenue for overcoming resistance in AML.

Materials and Methods

Cell lines and culture conditions

HEK-293T cells were grown in DMEM (Gibco) supplemented with 10% fetal bovine serum (FBS) and 1% penicillin-streptomycin. OCI-AML2 and OCI-AML3 AML cell lines were cultured in MEM Alpha medium (Gibco) with 10% FBS and 1% penicillin-streptomycin. Cas9-stable OCI-AML2 and OCI-AML3 lines were created by lentiviral introduction of lentiCas9-Blast (Addgene, 52962), followed by blasticidin selection and verification of Cas9 expression and activity. All cultures were incubated at 37°C with 5% CO_2. Periodic Mycoplasma testing ensured cell line integrity and authenticity.

Plasmid construction and sgRNA cloning

LentiCRISPR-V2 and Lenti-U6-sgRNA-puro-IRES-GFP plasmids were sourced from Addgene. Vectors were digested with BsmBI (NEB, R0580) for linearization and then ligated with designed sgRNA sequences using T4 DNA ligase (NEB, M0202V). The sgRNA sequences employed were: sgSC: 5′-AAACCCTATGCCCAAATGAG-3′; sgCHD7-1: 5′-TAGGATTCCCATCAAACAG-3′; sgCHD7-2: 5′-CACGTAGCACAGATGACCG-3′; sgANGPT1-1: 5′-ACGAGTAACCAAGCCTTGA-3′; sgANGPT1-2: 5′-TAATACAACATCGTGAAGA-3′. Complete plasmids were confirmed through Sanger sequencing before downstream applications.

Lentiviral production and cell transduction

Lentiviruses were packaged in HEK-293T cells by PEI (Polysciences, 23966-1) co-transfection of the transfer vector with packaging plasmids VSV-G and psPAX2. Viral supernatants were harvested 48 h later. Target cells were exposed to virus in medium containing 8 μg/mL polybrene (Beyotime, C0351) and spun at 1800 rpm for 60 min at room temperature. Medium was exchanged after 24 h, and selection antibiotics were added 48 h post-transduction. Knockout efficiency was validated by immunoblot analysis in every experiment.

CRISPR-based genetic screen and data processing

The pooled CRISPR library comprised sgRNAs targeting 1478 genes focused on transcription factors, kinases, and epigenetic regulators, originally assembled in the laboratories of Chunliang Li. Six sgRNAs per gene were included, plus 1000 non-targeting controls. OCI-AML2-Cas9 cells were transduced at low MOI (~0.3), selected with puromycin for 4 days, and then treated with DMSO or gilteritinib (200 nM or 1 μM) for 12 days while maintaining at least 1000× library coverage. Post-treatment, cells were collected, genomic DNA extracted, sgRNA regions amplified by PCR, and sequenced on the Illumina HiSeq 4000. Analysis was conducted using the MAGeCK algorithm.

Competitive growth assays (in vitro and in vivo)

For in vitro competition, AML cells transduced with GFP-linked individual sgRNAs were treated with drugs starting 4 days after transduction. The GFP-positive fraction was tracked by flow cytometry every 3 days, and values were normalized to the initial post-treatment measurement.

In vivo, control and CHD7-knockout OCI-AML2 cells were combined and transplanted into 6- to 8-week-old female NOD.Cg-Prkdcscid Il2rgtm1Wjl/SZJ NSG mice. Starting on day 7, mice received daily oral gilteritinib (20 mg/kg) or venetoclax (100 mg/kg) for one week. Weekly peripheral blood sampling allowed flow cytometric monitoring of population ratios. Two weeks after treatment began, GFP+ cell percentages were quantified in bone marrow, blood, and spleen. Mice were pathogen-free (negative for viral antibodies, Helicobacter hepaticus, and parasites) per health reports and sentinel testing. Procedures followed IACUC-approved protocols at Peking Union Medical College.

Cell viability testing and proliferation assessment

Control and CHD7-knockout cells were plated at 2700 cells/well in 96-well plates (triplicates). They were exposed for 3 days to dose ranges of gilteritinib (Sparkjade, SJ-mx0187), quizartinib (Sparkjade, SJ-MX0304), crenolanib (Sparkjade, SJ-MX0460), daunorubicin (Sparkjade, HY-13062), and venetoclax (MCE, HY-15531). Viability was determined with Cell Counting Kit-8 (Apexbio, K1018) per manufacturer instructions, measuring absorbance at 450 nm. Manual counts used trypan blue staining and a hemocytometer.

Side population detection

Cells were resuspended at 1×10^6 cells/mL in pre-warmed α-MEM with 2% FBS, stained with Hoechst 33342 (Beyotime, C1022) at 37°C for 90 min, washed, and counterstained with propidium iodide. Verapamil (50 μM; MCE, HY-1427) served as an efflux inhibitor. Analysis was performed on a BD FACSAria III flow cytometer (BD Biosciences, USA).

Colony formation assay

Methylcellulose (STEMCELL Technologies, 04230) was mixed with DMSO or 400 nM gilteritinib. 120 cells per condition were plated in 400 μL per well of 24-well plates. Colonies were counted after 10 days. Experiments were run in technical triplicates and repeated three independent times.

Protein immunoblotting

Cells were lysed in RIPA buffer with protease and phosphatase inhibitors plus phenylmethylsulfonyl fluoride after PBS washing. Lysates were centrifuged at 12,000 × g (10 min, 4°C), quantified, and denatured at 100°C for 10 min. Proteins were separated by SDS-PAGE, transferred to PVDF membranes, blocked with 5% nonfat milk in TBST (1 h, room temperature), and incubated overnight at 4°C with antibodies to β-actin (Santa Cruz, sc-47778), CHD7 (Abcam, ab307499), P-ERK (Cell Signaling Technology, 9101S), P-AKT (Cell Signaling Technology, 9271S), ERK (Cell Signaling Technology, 9102S), AKT (Cell Signaling Technology, 9272S), P-STAT5 (Sangon Biotech, D155020), P-p65 (Sangon Biotech, D155006), STAT5A (Sangon Biotech, D220085-0025), p65 (Sangon

Biotech, D220135), and ANGPT1 (Sangon Biotech, D120216). After TBST washes, HRP-secondary antibodies were applied for 1 h at room temperature, followed by ECL detection (YEASEN, 36208ES60).

Flow cytometry applications

GFP-positive cell percentages were measured after pelleting cells (300 × g, 5 min), resuspending in PBS, and adding DAPI for viability gating on an LSRFortessa (BD Biosciences). Apoptosis was assessed after 3-day treatment with 400 nM gilteritinib or 20 nM venetoclax using annexin V-FITC/PI staining (YEASEN, 40302ES60). Mitochondrial membrane potential was evaluated post-treatment by JC-1 staining (Beyotime, C2003S) at 37°C for 20 min in 500 μL α-MEM, followed by two washes (600 × g, 4 min) and flow cytometric analysis. Data processing used FlowJo software (Tree Star).

RNA isolation, reverse transcription, and transcriptomic profiling

Cellular RNA was purified using the RNeasy kit (Sparkjade, AC0205-B) as directed by the manufacturer. First-strand cDNA was generated from the purified RNA with Hifair 1st Strand cDNA Synthesis SuperMix (YEASEN, 11141ES60). Quantitative PCR amplification was conducted in technical triplicates employing Hieff UNICON Universal Blue qPCR SYBR Green Master Mix (YEASEN, 11184ES08) on a QuantStudio 5 instrument (Thermo Fisher Scientific). Relative transcript abundance was quantified via the ΔΔ-CT approach, with normalization to β-actin. Primer pairs utilized were: β-actin forward 5′-CATGTACGTTGCTATCCAGGC-3′ and reverse 5′-CTCCTTAATGTCACGCACGAT-3′; GAPDH forward 5′-CGGGAAACTGTGGCGTGAT-3′ and reverse 5′-AGTGGGTGTCGCTGTTGAAGT-3′; FLT3 forward 5′-AGGGACAGTGTACGAAGCTG-3′ and reverse 5′-GCTGTGCTTAAAGACCCAGAG-3′; ANGPT1 forward 5′-AGCGCCGAAGTCCAGAAAAC-3′ and reverse 5′-TACTCTCACGACAGTTGCCAT-3′.

RNA-seq libraries were sequenced on the Illumina NovaSeq X Plus platform following established workflows. Following alignment and quantification, read counts were normalized using DESeq2 (version 2.2.1). Differentially expressed genes were subsequently identified through integration with the limma package (version 3.58.1).

Proteomic sample preparation and mass spectrometry

Proteins were isolated from the matched samples utilized for RNA-seq analysis via the EasyPep™ Mini MS Sample Prep Kit (Cat. No. A40006) according to the provided protocol. Total protein content was quantified with the Pierce™ BCA Protein Assay Kit (Cat. No. 23227). Resulting peptides were separated and analyzed by LC-MS/MS on a Thermo Scientific Orbitrap Exploris 480 mass spectrometer interfaced with a Vanquish Flex UHPLC system in data-independent acquisition (DIA) mode. Spectral data processing was performed with DIA-NN (version 1.9.1) in library-free search mode against the UniProt human database, using a 60-minute gradient. Identifications were filtered at a 1% false discovery rate (FDR). Imputation of missing values employed the sequential k-nearest neighbors (seq-knn) approach on the NAguideR platform [33, 34]. Protein intensities were subjected to median normalization. Differential abundance analysis was executed in R using limma (version 3.58.1), defining differentially expressed proteins (DEPs) as those with $\log FC > 0$ and $p < 0.05$. Overlap with core pathway components was then examined. All analyses were conducted in R environment (version 4.3.1).

Weighted gene co-expression network construction

Co-expression networks were built using the WGCNA R package (version 1.73) on the most variably expressed genes based on logCPM values. Outlier samples were identified and removed according to sample clustering results. The soft-threshold power β was determined to approximate scale-free network topology. An unsigned topological overlap matrix (TOM) was computed, followed by hierarchical clustering to define modules. Similar modules were merged based on eigengene dissimilarity. Module membership strength was evaluated by kME values. Functional annotation of modules was performed via KEGG enrichment analysis with clusterProfiler (version 4.10.1). Candidate hub genes were derived by cross-referencing WGCNA modules with differentially expressed gene lists.

Chromatin accessibility profiling by ATAC-seq

ATAC-seq experiments were executed using the Hyperactive ATAC-Seq Library Prep Kit for Illumina (Vazyme, TD711) on 1×10^5 cells per sample, following the recommended protocol. Sequencing was carried out on the

Illumina NovaSeq X Plus platform. Raw reads were processed for quality control and adapter trimming with fastp (v0.23.2). Alignment to the hg38 genome was performed with bowtie2 (v2.4.5). Duplicate reads were marked and removed using sambamba, and low-quality alignments filtered with samtools. Peak detection utilized MACS2 (v2.2.7.1). Genomic visualizations were generated with pyGenomeTracks (v3.5.1).

Mining of external genomic and clinical datasets

Gene effect scores (Chronos) for FLT3 and corresponding expression data in AML cell lines were downloaded from the DepMap portal (https://depmap.org/portal/interactive/). Associations between FLT3 transcript levels and essentiality scores were evaluated by Pearson correlation.

AML patient clinical information was accessed through the UCSC Xena platform (http://xena.ucsc.edu/). The relationship between CHD7 expression and overall survival (OS) was examined using Kaplan-Meier analysis implemented in the survival R package (version 4.3.2). RPKM-normalized expression values for CHD7 and ANGPT1 were retrieved from the Beat AML dataset (http://vizome.org/aml/). Correlation between these genes was computed using the cor.test function in R (version 4.3.2).

Public CUT&RUN and ChIP-seq datasets were obtained from GEO (https://www.ncbi.nlm.nih.gov/geo/) and ENCODE (https://www.encodeproject.org) under the accessions GSE171136, GSE108506, and ENCSR000AVA. Integrated visualization of these datasets was achieved with pyGenomeTracks (v3.5.1).

Statistical evaluation

Statistical testing was performed in GraphPad Prism. Two-group comparisons were analyzed by unpaired t-test, and multi-group differences by one-way ANOVA. KEGG pathway enrichment significance was calculated using the hypergeometric test in clusterProfiler. Survival differences were assessed by log-rank test on Kaplan-Meier curves generated with the survival package in R (version 4.3.2). Results from dose-response (IC50), apoptosis, proliferation, and competition experiments are expressed as mean ± standard error of the mean (SEM) from at least three biological replicates. Significance levels are marked in figures as follows: ns ($p \geq 0.05$), *$p < 0.05$, **$p < 0.01$, ***$p < 0.001$.

Results and Discussion

CRISPR-Cas9 screen identifies CHD7 as a novel regulator of gilteritinib resistance in AML cells

Gilteritinib, an FLT3 inhibitor approved for clinical use in relapsed/refractory (R/R) AML [35], was the focus of this investigation. To discover genes modulating cellular responsiveness to this therapy, correlations between FLT3 transcript levels and CRISPR essentiality scores were systematically explored across a panel of AML cell lines in the DepMap database [36]. OCI-AML2 cells were chosen for the primary CRISPR-Cas9 screen owing to their strong FLT3 expression and partial dependence on this pathway for survival. The custom sgRNA library targeted 1478 genes with six guides each and incorporated 1000 non-targeting controls. After stable transduction and selection, cells underwent 12-day exposure to DMSO vehicle or gilteritinib (200 nM or 1 μM) to enable outgrowth of resistant populations through repeated cell divisions. Genomic DNA extracted at the endpoint was deeply sequenced **(Figure 1a)**, and sgRNA abundance changes were analyzed via the MAGeCK algorithm at a significance level of $p < 0.05$ [37].

This approach successfully recovered known resistance mediators such as BCOR, CHD1, and PPP2CA, validating screen performance **(Figures 1b and 1c)** [38-40]. Notably, CHD7 emerged as a top hit, with its knockout strongly promoting survival under gilteritinib treatment at both concentrations. All five CHD7-directed sgRNAs were markedly enriched in drug-treated conditions **(Figure 1d)**, demonstrating highly reproducible effects. Although CHD7 had not been previously connected to drug resistance, analysis of TCGA-LAML patient data revealed that lower CHD7 expression associated with inferior survival outcomes **(Figure 1e**), supporting its clinical relevance in AML.

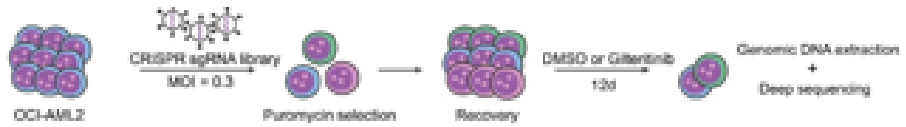

a)

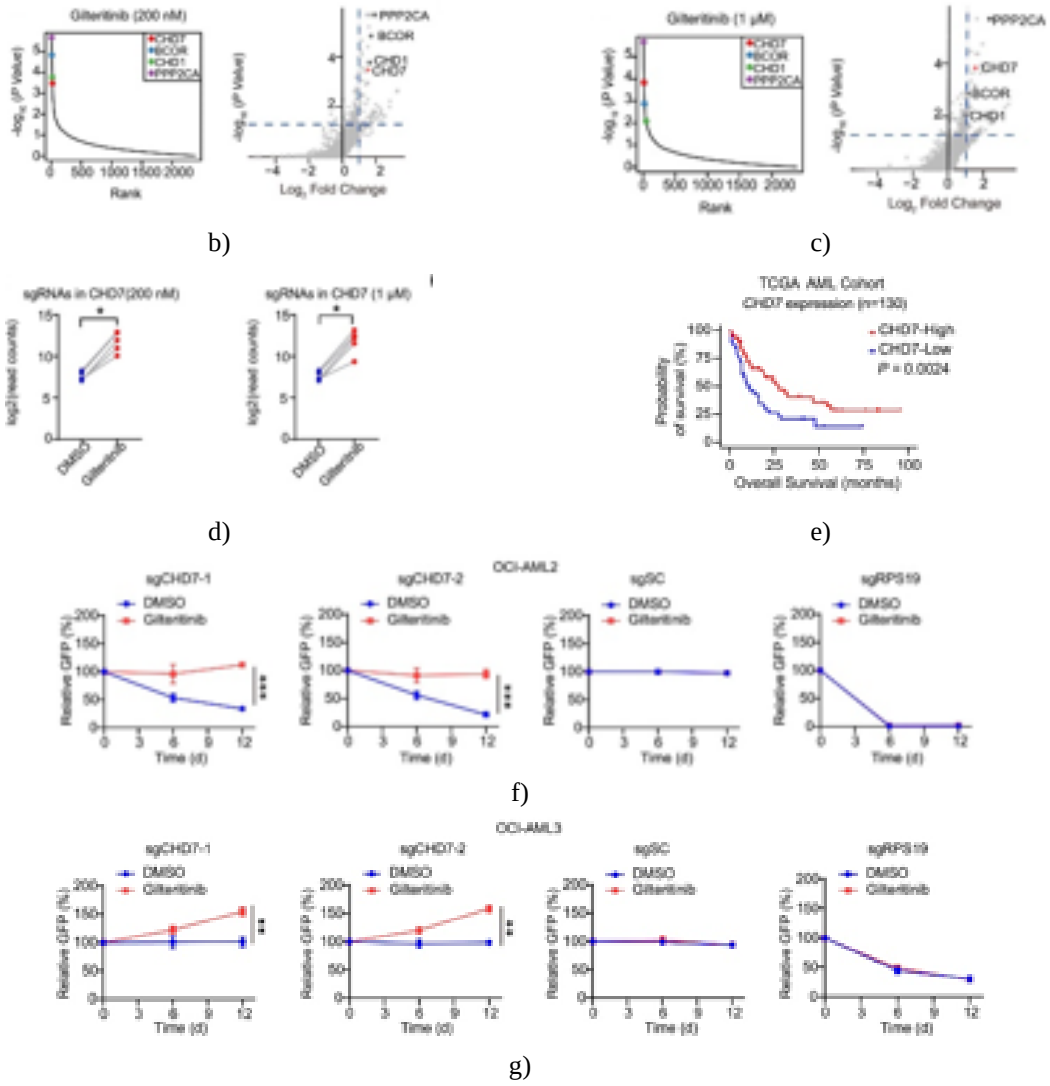

Figure 1. CRISPR-Cas9 knockout screen identifies CHD7 as a novel regulator of gilteritinib resistance in AML cells. (a) Experimental design of the CRISPR-Cas9-based screen to identify genes whose inactivation drives gilteritinib resistance in OCI-AML2 cells. (b, c) MAGeCK-derived enrichment scores (left) and volcano plots (right) comparing vehicle versus gilteritinib (200 nM and 1 μM) conditions on the basis of log10 (p-value), highlighting CHD7 in red. (d) Normalized read counts for individual sgRNAs targeting CHD7. $p < 0.05$. (e) Kaplan-Meier survival plot of AML patients (n = 130) grouped by CHD7 expression status, with log-rank test $p = 0.0024$. (f, g) Competitive proliferation experiments tracking GFP-positive fractions in OCI-AML2 (400 nM gilteritinib) and OCI-AML3 (600 nM gilteritinib) cells expressing sgRNAs. Scramble sgRNA (sgSC) served as negative control and RPS19-targeted sgRNA (sgRPS19) as positive lethality control. Percentages were normalized to initial time points. AML, acute myeloid leukemia; sgRNAs, single guide RNAs. $^{**}p < 0.01$, $^{***}p < 0.001$.

To confirm the contribution of CHD7 to the therapeutic sensitivity of AML cells toward gilteritinib, competitive proliferation assays were carried out using the OCI-AML2 and OCI-AML3 cell lines. Two potent sgRNAs specific for CHD7 (sgCHD7-1 and sgCHD7-2) were utilized, alongside a scrambled sgRNA (sgSC) as the negative control and an sgRNA against the essential survival gene RPS19 (sgRPS19) as the positive control to evaluate lethality following gene knockout. After exposure to gilteritinib, cells harboring CHD7-targeting sgRNAs demonstrated a clear selective growth advantage relative to non-transduced cells, in contrast to the scramble sgRNA controls, which displayed no such benefit; this outcome corroborated the original screening data **(Figures 1f and 1g)**. In parallel, loss of BCOR or PPP2CA similarly promoted resistance to gilteritinib, thereby strengthening the validity of the observed effects. Recognizing the shared molecular features between AML and

chronic myeloid leukemia (CML), the experiments were extended to K562 cells to determine whether CHD7 inactivation would exert analogous effects on gilteritinib responsiveness in this CML model. As seen in AML cells, CHD7 depletion in K562 cells led to elevated resistance against gilteritinib, pointing to a preserved mechanism by which CHD7 influences drug sensitivity in diverse leukemia settings. In summary, these data establish CHD7 as an important mediator of gilteritinib resistance in AML and indicate its value as a potential target for strategies aimed at reversing therapeutic resistance.

Loss of CHD7 induces resistance to FLT3 inhibitors in AML cells

Stable CHD7-knockout OCI-AML2 cell lines were generated to further characterize this phenotype. Efficient protein depletion was confirmed by immunoblot **(Figure 2a)**. CHD7-deficient cells displayed substantially elevated IC50 values for gilteritinib compared with sgSC controls **(Figure 2b)**. Parallel resistance was documented in additional lines including OCI-AML3, K562, MV4-11, and HL-60.

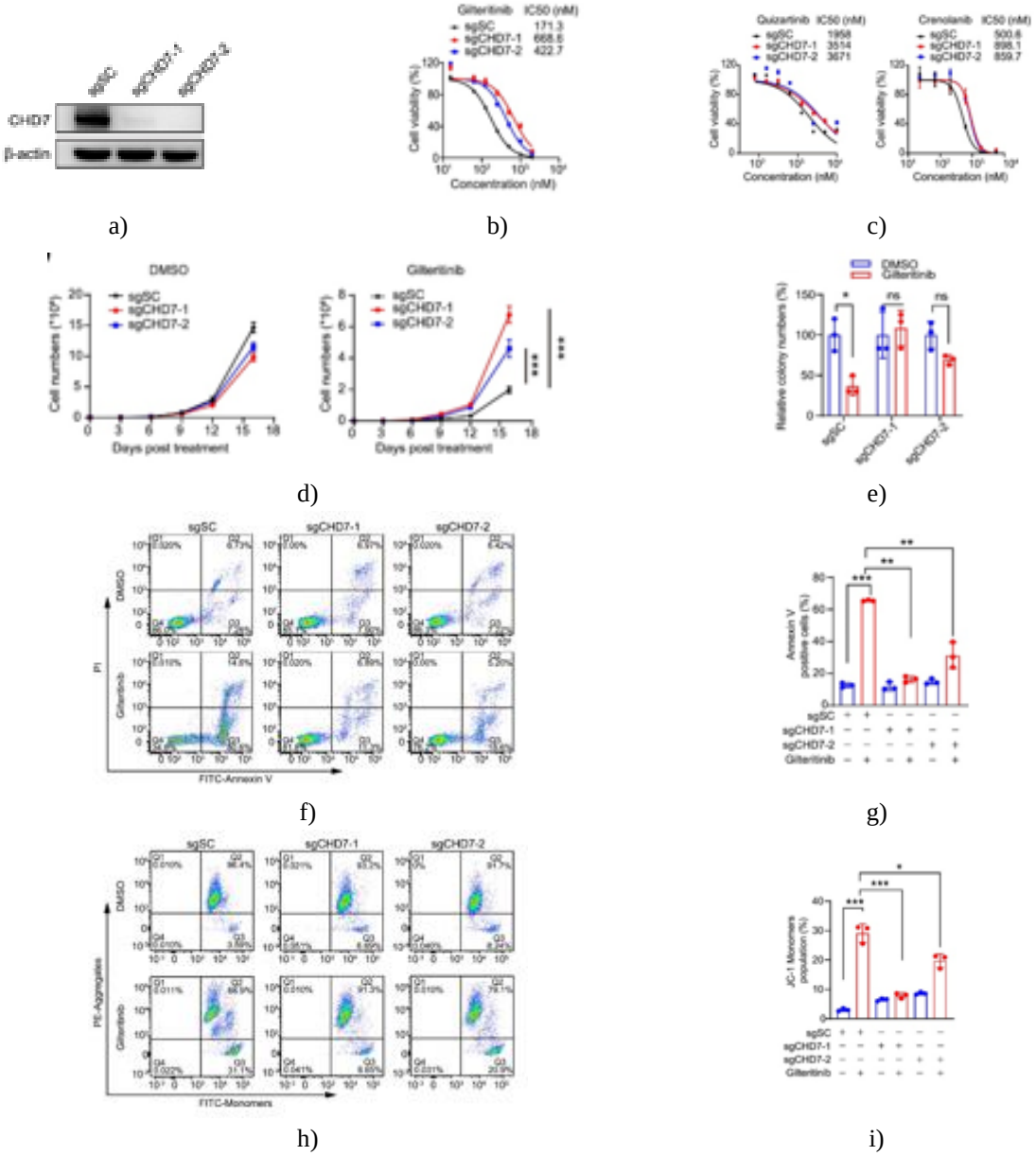

Figure 2. CHD7 knockout confers resistance to multiple FLT3 inhibitors in AML cells. (a) Immunoblot verification of CHD7 knockout in OCI-AML2 cells. (b, c) Viability dose-response curves for sgRNA-expressing OCI-AML2 cells treated for 3 days with DMSO or graded concentrations of gilteritinib, quizartinib, or crenolanib. Data normalized to DMSO. (d) Cell proliferation monitored by viable cell counts

every 3–4 days in the presence of DMSO or 400 nM gilteritinib. Mean ± SEM from three experiments. ***p < 0.001. (e) Colony-forming capacity of the indicated sgRNA lines in methylcellulose with DMSO or 400 nM gilteritinib after 10 days. *p < 0.05. (f, g) Apoptosis rates assessed by Annexin-V/PI staining after 3-day DMSO or 400 nM gilteritinib exposure. Mean ± SEM of three replicates. **p < 0.01, ***p < 0.001. (h, i) JC-1-based measurement of mitochondrial membrane potential dissipation following 3-day treatment. Mean ± SEM of three replicates. AML, acute myeloid leukemia; sgRNAs, single guide RNAs. *p < 0.05, ***p < 0.001.

To further investigate the consequences of CHD7 depletion on sensitivity to additional FLT3 inhibitors, quizartinib and crenolanib—both of which have shown clinical efficacy against AML through FLT3 targeting [41, 42]—we conducted parallel experiments. In agreement with the observations for gilteritinib, cells lacking CHD7 also displayed resistance to quizartinib and crenolanib **(Figure 2c)**. Furthermore, serial cell counting performed at 3–4 day intervals demonstrated that CHD7-knockout cells proliferated more rapidly than control cells when cultured in gilteritinib-supplemented medium **(Figure 2d)**. Supporting these observations, clonogenic assays indicated a substantially greater colony-forming capacity in CHD7-deficient cells under gilteritinib exposure **(Figure 2e)**. We additionally examined the potential influence of CHD7 loss on leukemia stem cell-like characteristics via the side population (SP) assay. CHD7 knockout produced no significant change in the SP fraction, implying that the acquired drug resistance is not primarily attributable to alterations in stemness properties. To more directly examine the role of CHD7 in modulating gilteritinib-triggered cell death, flow cytometric analysis with FITC-Annexin V/PI staining was performed, revealing a pronounced decrease in apoptotic cells among CHD7-depleted AML populations **(Figures 2f and 2g)**. Consistent with this, JC-1 staining indicated that CHD7 knockout cells experienced markedly reduced dissipation of mitochondrial membrane potential after gilteritinib treatment relative to controls **(Figures 2h and 2i)**. Taken together, these results indicate that CHD7 depletion promotes resistance to FLT3 inhibitors in AML cells through enhanced proliferation, increased colony-forming ability, and attenuation of apoptosis.

Loss of CHD7 confers multi-drug resistance in AML cells

Further experiments addressed whether CHD7 inactivation leads solely to FLT3 inhibitor resistance or generates a wider spectrum of chemoresistance. CHD7-deficient AML cells exhibited pronounced resistance to venetoclax, the BCL-2 antagonist often paired with hypomethylating agents for initial AML treatment [43-45]. This phenotype included higher IC50 values and faster outgrowth when exposed to venetoclax **(Figures 3a and 3b)**. Analogous effects appeared with daunorubicin, an early-generation anthracycline [46, 47], manifesting as increased IC50 and superior proliferative capacity in knockout cells versus controls **(Figures 3c and 3d)**. Reduced apoptotic fractions were evident after venetoclax challenge in CHD7-depleted populations, reaching nearly half the level seen in controls **(Figures 3e and 3f)**. Mitochondrial integrity was better maintained in these cells, as shown by limited membrane potential collapse **(Figures 3g and 3h)**. Decreased caspase-3 processing after venetoclax addition provided additional evidence of blunted cell death signaling. In summary, CHD7 loss promotes broad chemoresistance in AML that encompasses FLT3-directed therapies and multiple standard agents.

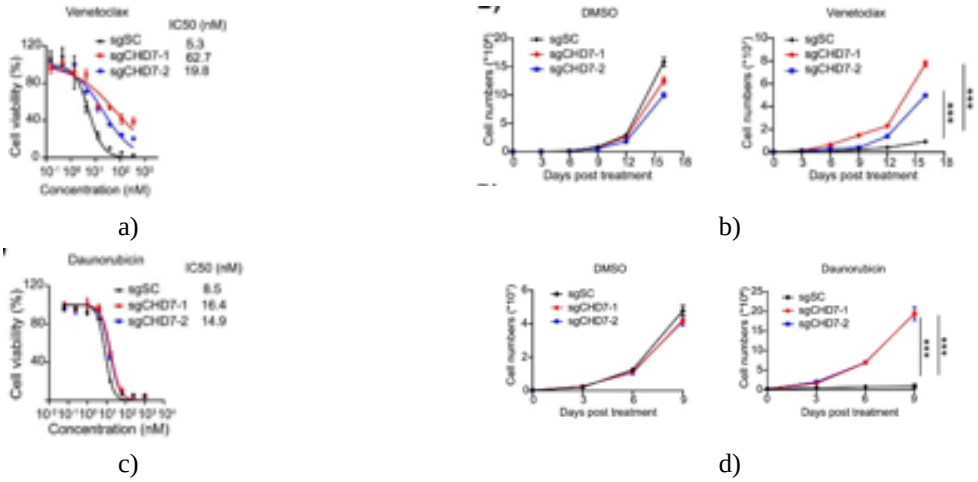

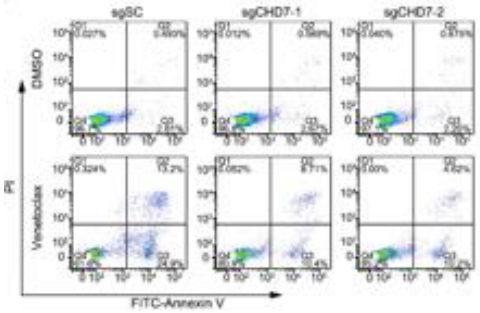

e)

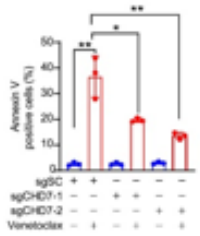

f)

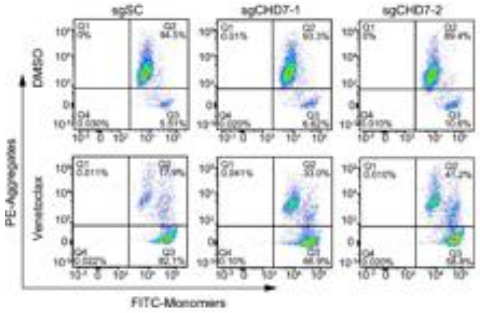

g)

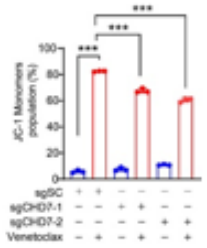

h)

Figure 3. Loss of CHD7 reduces the cytotoxic effects of multiple AML therapeutics. (a) Dose-dependent viability of OCI-AML2 cells with different sgRNAs after venetoclax exposure, quantified by CCK-8 assay. Values indicate mean ± SEM across three replicates. (b) Longitudinal viable cell counts in OCI-AML2 cultures expressing the indicated sgRNAs under DMSO or 20 nM venetoclax. Data are mean ± SEM from three experiments. ***p < 0.001. (c) Dose-dependent viability of OCI-AML2 cells with different sgRNAs after daunorubicin exposure, quantified by CCK-8 assay. (d) Longitudinal viable cell counts in OCI-AML2 cultures expressing the indicated sgRNAs under DMSO or 10 nM daunorubicin. Data are mean ± SEM from three experiments. ***p < 0.001. (e, f) Apoptotic cell percentages determined by Annexin-V/PI staining in OCI-AML2 cells with the indicated sgRNAs following 3-day DMSO or 20 nM venetoclax treatment. Data are mean ± SEM from three replicates. *p < 0.05, **p < 0.01. (g, h) JC-1 assay results showing mitochondrial membrane potential status in OCI-AML2 cells with the indicated sgRNAs after 3-day DMSO or 20 nM venetoclax treatment. Data are mean ± SEM from three replicates. AML, acute myeloid leukemia; sgRNAs, single guide RNAs. ***p < 0.001.

Loss of CHD7 impairs sensitivity of AML to gilteritinib and venetoclax in vivo

The in vivo consequences of CHD7 loss on drug sensitivity were evaluated using a xenograft approach. OCI-AML2 cells were introduced into NSG recipients. A competitive mixture was prepared by combining GFP-marked CHD7-targeted cells with unmarked Cas9-expressing cells at a 1:3 ratio (~30% GFP+ to 70% GFP−). Drug administration began seven days after transplantation, consisting of daily oral gilteritinib (20 mg/kg) or venetoclax (100 mg/kg) for seven days. Tissue analysis occurred two weeks after treatment onset **(Figure 4a)**. Treatment with either agent led to substantial enrichment of GFP-positive CHD7-knockout cells within the CD45+ leukemic compartment in bone marrow, blood, and spleen relative to vehicle controls **(Figures 4b and 4c)**. These results establish that CHD7 deficiency reduces drug effectiveness and favors leukemia cell dominance under therapeutic selection in living organisms.

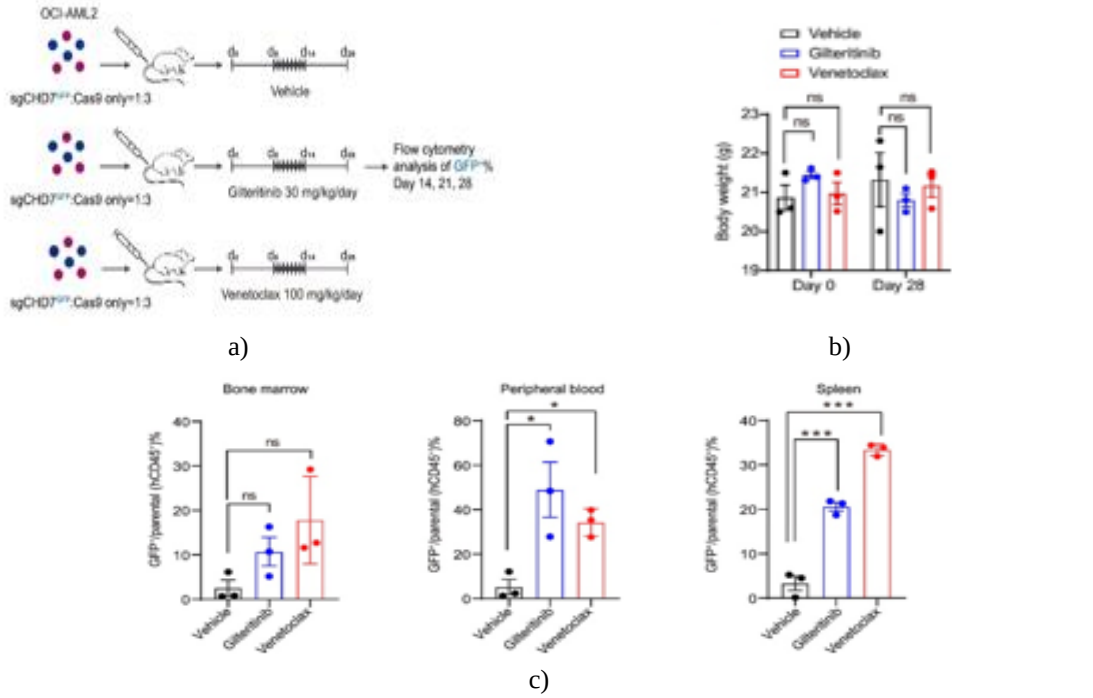

a) b) c)

Figure 4. CHD7 knockout decreases AML sensitivity to gilteritinib and venetoclax in vivo. (a) Outline of the competitive xenograft proliferation experiment. (b) Recorded body weights during vehicle, gilteritinib, or venetoclax administration. (c) Percentage of GFP-tagged sgCHD7 cells detected by flow cytometry in bone marrow, peripheral blood, and spleen (n = 3 mice per group). AML, acute myeloid leukemia. *p < 0.05, ***p < 0.001.

Multi-omics analyses reveal that CHD7 loss enhances the activation of PI3K/AKT and MAPK/ERK pathways

Mechanistic insights into CHD7-associated resistance were pursued through parallel transcriptomic and proteomic profiling of control and CHD7-knockout OCI-AML2 cells, with and without drug exposure **(Figure 5a)**. WGCNA clustering produced 12 gene co-expression modules. The blue module displayed strong induction in knockout samples, while the turquoise module was largely suppressed **(Figure 5b)**. Module expression trends and representative high-membership genes are shown in box plots **(Figure 5c)**.

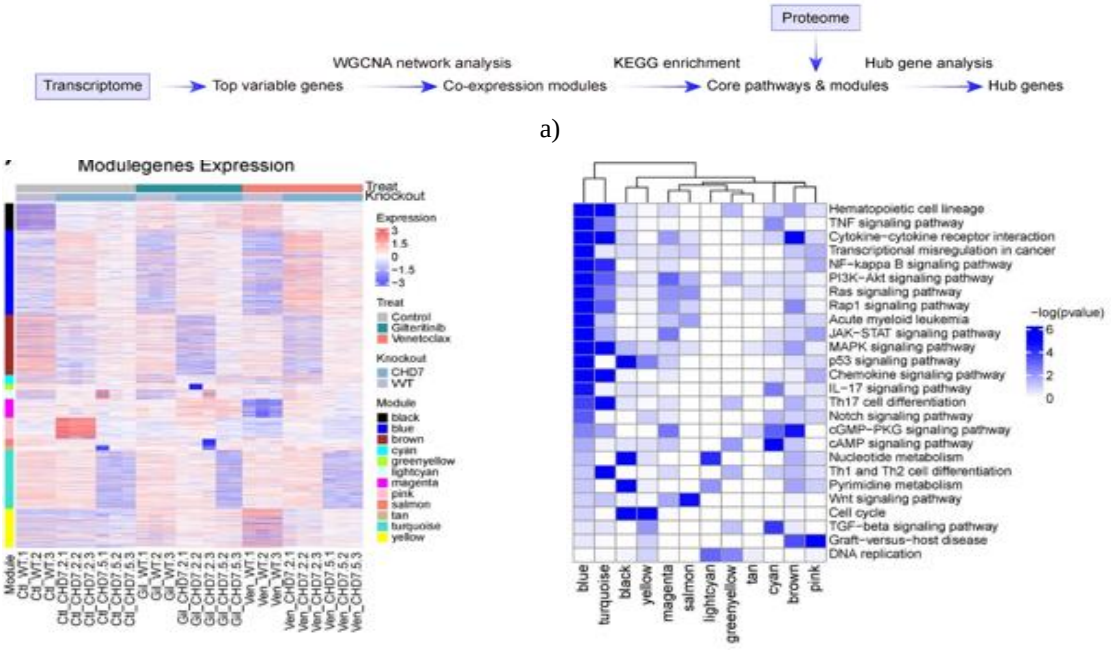

a) b) d)

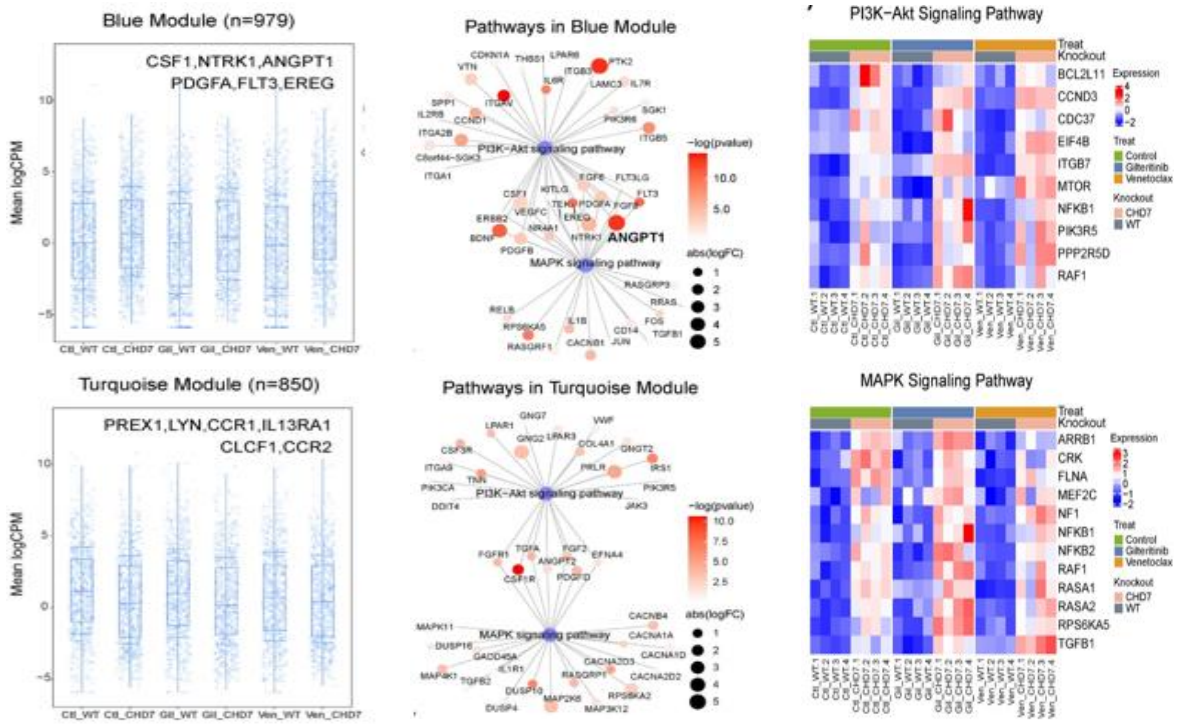

c) e) f)

Figure 5. Multi-omics analysis reveals that CHD7 loss enhances the activation of PI3K/AKT and MAPK/ERK pathways. (a) Schematic of the multi-omics integration strategy. (b) Expression heatmap of the 12 modules across experimental conditions (control or CHD7 depletion combined with DMSO, gilteritinib, or venetoclax). Enrichment p-values were calculated by hypergeometric test (threshold $p < 0.05$). (c) Boxplots of expression distributions for the blue (top) and turquoise (bottom) modules. Core genes with kME > 0.8 are labeled. (d) KEGG enrichment analysis of genes belonging to the detected modules. (e) Network diagram linking genes in PI3K/AKT and MAPK/ERK pathways from the blue module (top) and turquoise module (bottom). Node color corresponds to adjusted p-value and size to log2 fold change. (f) Heatmap of proteins upregulated in both transcriptomic and proteomic datasets within the PI3K/AKT and MAPK/ERK cascades.

Pathway analysis highlighted enrichment of hematopoietic and AML-related processes in the altered modules, consistent with known contributions of CHD7 to blood cell maturation and oncogenic transformation [24, 28]. Prominent enrichment was also observed for NF-κB, PI3K/AKT, MAPK/ERK, JAK/STAT, and P53 signaling, suggesting their participation in CHD7-governed drug responses **(Figure 5d)**.

Hub gene analysis within the PI3K/AKT and MAPK/ERK networks highlighted ANGPT1 as the most strongly induced candidate, indicating a pivotal position in the altered signaling landscape **(Figure 5e)**. Proteomics data showed matching elevations in protein abundance for key pathway members, demonstrating alignment between mRNA and protein changes **(Figure 5f)**. These results collectively point to upregulated PI3K/AKT and MAPK/ERK activity as a central driver of the resistance state triggered by CHD7 inactivation.s

The CHD7-ANGPT1 axis promotes multidrug resistance in AML

Immunoblotting experiments provided further confirmation of the pathways controlled by CHD7. Inactivation of CHD7 counteracted the downregulation of AKT, ERK, and p65 phosphorylation that normally occurs upon exposure to gilteritinib or venetoclax **(Figure 6a)**. Although gene expression profiling pointed to possible JAK-STAT involvement, phosphorylation of STAT5 remained largely unchanged at the protein level, arguing against meaningful activation of this route. FLT3 expression itself was not elevated following CHD7 loss; modest reductions were instead detected at both mRNA and protein levels in OCI-AML2 cells. Despite this, downstream FLT3 signaling through P-AKT and P-ERK proved less effectively inhibited by gilteritinib in the absence of CHD7. The resistance mechanism therefore appears rooted in broader reprogramming of PI3K/AKT, MAPK/ERK, and NF-κB networks.

ANGPT1 represented a standout candidate within these alterations. The protein product of ANGPT1 is a secreted factor that engages the TIE2 receptor, inducing dimerization and tyrosine phosphorylation to stimulate PI3K/AKT and MAPK/ERK cascades [48, 49]. CHD7 deletion led to clear upregulation of ANGPT1 at both transcript and protein levels **(Figures 6b and 6c)**. As a chromatin remodeler, CHD7 likely influences ANGPT1 transcription directly. ATAC-seq profiling in knockout versus control cells uncovered increased chromatin accessibility at the ANGPT1 promoter and enhancer elements, matching the observed rise in mRNA **(Figure 6d)**. Independent ChIP-seq and CUT&RUN datasets (GSE171136 [50], GSE108506 [51], ENCSR000AVA [52]) revealed CHD7 occupancy at the ANGPT1 promoter in multiple cellular contexts. Patient data from the Beat-AML collection additionally showed an inverse association between CHD7 and ANGPT1 expression **(Figure 6e)**. These results position ANGPT1 as a functionally relevant target of CHD7 whose derepression contributes to the resistant phenotype.

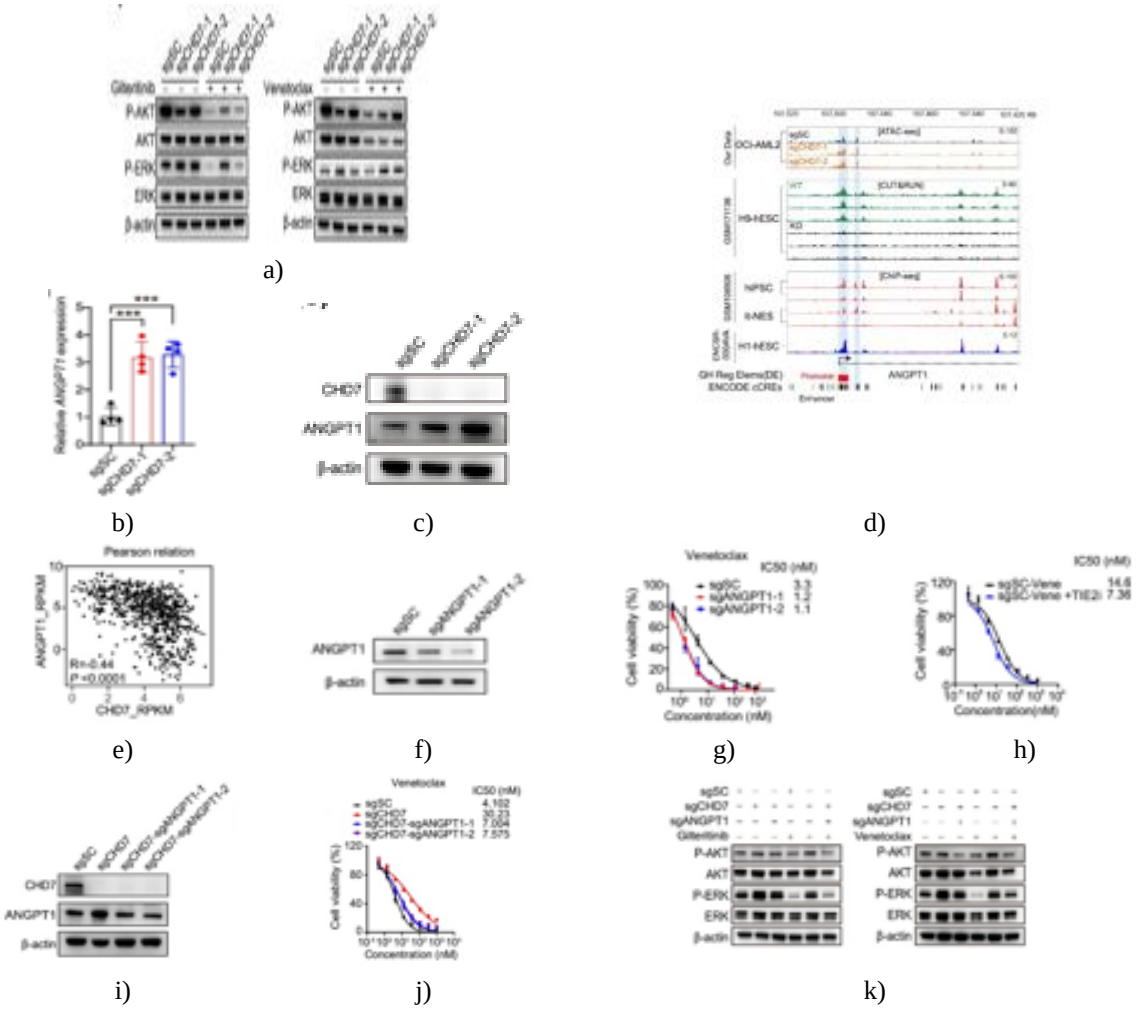

Figure 6. ANGPT1 knockdown partially restores drug sensitivity in CHD7-deficient AML cells. (a) Western blot analysis of P-AKT, AKT, P-ERK, and ERK proteins in OCI-AML2 cells with the indicated sgRNAs after 48 h of gilteritinib or venetoclax treatment. (b) Quantification of ANGPT1 mRNA by RT-PCR in control versus CHD7-depleted OCI-AML2 cells. ***$p < 0.001$. (c) Western blot detection of CHD7 and ANGPT1 proteins in control and CHD7-depleted OCI-AML2 cells. (d) Browser tracks from ATAC-seq and public CHD7 CUT&RUN/ChIP-seq experiments showing altered chromatin accessibility and binding at the ANGPT1 locus. (e) Correlation between CHD7 and ANGPT1 mRNA levels in Beat-AML patient samples. (f) Western blot confirming ANGPT1 protein reduction after knockdown. (g) Dose-response viability curves for OCI-AML2 cells with the indicated sgRNAs following 3-day venetoclax exposure, normalized to DMSO. (h) Viability measured by CCK-8 after venetoclax treatment alone or combined with 2 μM TIE2 kinase inhibitor. (i) Western blot verification of ANGPT1 knockdown efficiency in CHD7-deficient background. (j)

CCK-8 viability assay in the indicated sgRNA lines after 3-day venetoclax treatment. (k) Western blot analysis of P-AKT/AKT and P-ERK/ERK in cells expressing different sgRNAs treated for 24 h with 400 nM gilteritinib or 20 nM venetoclax. AML, acute myeloid leukemia; sgRNAs, single guide RNAs.

Depletion of ANGPT1 using independent sgRNAs **(Figure 6f)** sensitized cells to venetoclax and lowered the IC50 **(Figure 6g)**. Chemical inhibition of TIE2 with the corresponding kinase inhibitor [53] produced a similar sensitization effect **(Figure 6h)**. In CHD7-knockout cells, ANGPT1 knockdown partially reversed resistance to venetoclax **(Figures 6i and 6j)** and decreased downstream AKT and ERK phosphorylation during drug treatment **(Figure 6k)**.

Pharmacological inhibition of ANGPT1-TIE2 signaling overcomes CHD7 mediated drug resistance in AML

To explore clinical translation, CHD7-knockout OCI-AML2 cells were exposed to gilteritinib or venetoclax combined with TIE2 kinase inhibitor 1. The dual regimens achieved stronger growth suppression and greater IC50 reductions than either drug alone **(Figure 7a)**. Phosphorylation of AKT and ERK was also more effectively blocked by the combinations **(Figure 7b)**. These observations highlight TIE2 pathway blockade as a potential means to bypass CHD7-associated resistance.

Testing in primary patient-derived AML blasts (both FLT3 wild-type and FLT3-ITD) confirmed that adding TIE2i to gilteritinib or venetoclax enhanced cytotoxicity compared with single agents. Low doses of TIE2i displayed minimal standalone toxicity **(Figures 7c and 7d)**, supporting an acceptable therapeutic index. Overall, targeting the ANGPT1-TIE2 axis emerges as a valuable strategy for counteracting multidrug resistance in AML driven by CHD7 loss **(Figure 7e)**.

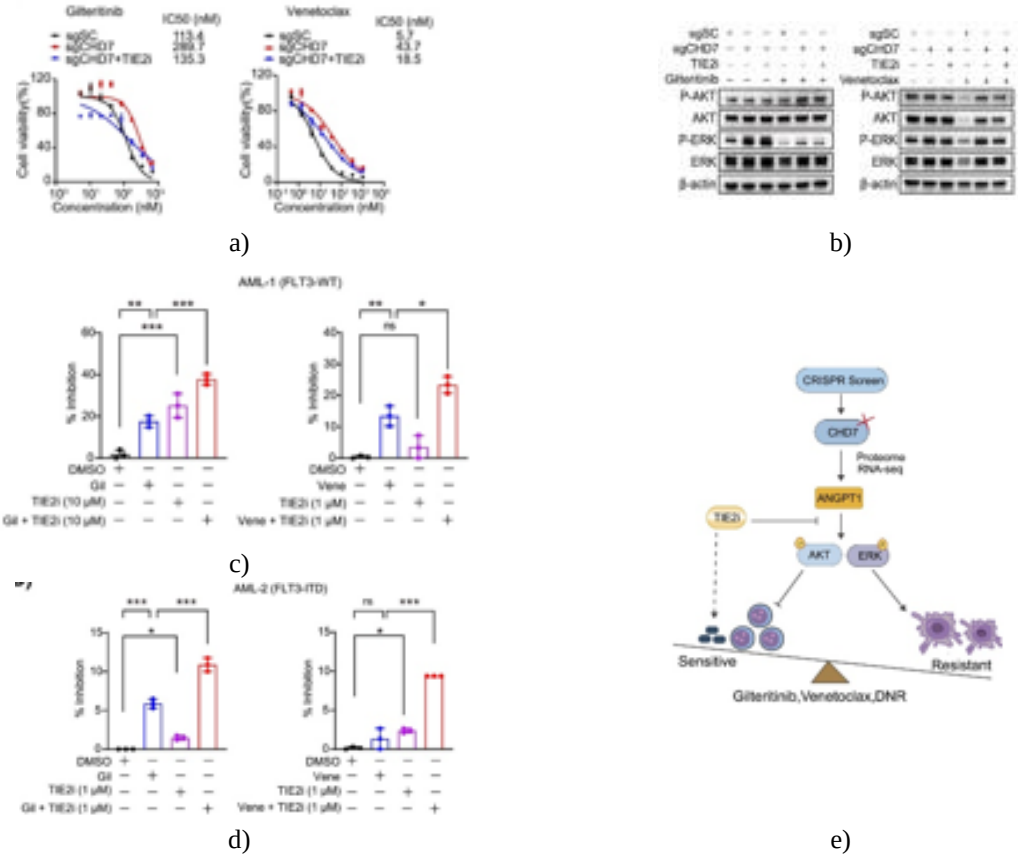

Figure 7. Pharmacological inhibition of ANGPT1-TIE2 signaling overcomes CHD7 mediated drug resistance in AML. (a) CCK-8 viability assay in OCI-AML2 cells with indicated sgRNAs after 3-day treatment with gilteritinib or venetoclax, alone or plus 2 μM TIE2i. (b) Western blots of P-AKT, AKT, P-ERK, and ERK in sgRNA-expressing cells treated for 24 h with 400 nM gilteritinib or 20 nM venetoclax, with or without 2 μM TIE2i. (c, d) Viability of primary AML blasts from two patients treated for 72 h with gilteritinib (Gil) or venetoclax (Vene) monotherapy versus combination with TIE2i. Inhibition rates were calculated from CCK-8 readings. FLT3-WT AML-1: 200 nM gilteritinib, 100 nM venetoclax. FLT3-ITD

AML-2: 100 nM gilteritinib, 100 nM venetoclax. *p < 0.05, **p < 0.01, ***p < 0.001. (e) Diagram summarizing the CHD7-ANGPT1 regulatory axis and its impact on therapeutic resistance in AML. AML, acute myeloid leukemia; sgRNAs, single guide RNAs.

Taken together, and drawing an analogy to the established "oncogene" and "tumor suppressor" paradigms in cancer development, this investigation establishes the CHD7-ANGPT1 partnership as a new "drug resistance suppressor" in acute myeloid leukemia (AML).

AML is the predominant leukemia affecting adults and carries a high incidence. Despite substantial progress in targeted therapies, which have enhanced survival and remission rates, the emergence of drug resistance and disease relapse continues to represent formidable obstacles [3, 54, 55]. Gilteritinib and venetoclax, recently approved by the FDA, exhibit wide-ranging clinical activity [6]. However, acquired resistance to these agents remains a persistent clinical problem. The continued refinement of deep sequencing methods alongside the growing deployment of CRISPR-Cas9 functional genomic screens has opened avenues for discovering novel molecular targets that can illuminate mechanisms of resistance to targeted therapies [56-59].

Using a genome-wide CRISPR-Cas9 knockout screen, we systematically evaluated mediators of gilteritinib resistance in AML and pinpointed CHD7 as a critical factor; its inactivation promoted resistance to several agents, most prominently gilteritinib and venetoclax. CHD7 is a member of the chromodomain helicase DNA-binding (CHD) protein family and is involved in multiple fundamental cellular processes [60], such as transcriptional control, DNA damage repair, embryonic organogenesis, and malignant transformation [61-63]. This factor is indispensable for proper development of embryonic tissues, especially those of neuronal and hematopoietic origin. Mutations that impair CHD7 function expand hematopoietic stem and progenitor cell (HSPC) populations and favor myeloid lineage commitment [24, 64]. Furthermore, aberrant CHD7 expression levels play important roles across several cancer types. Reduced CHD7 promotes open chromatin states that enable BMI1-mediated repression of DUSP4, an inhibitor of ERK, thereby driving ERK hyperactivation and accelerated proliferation in medulloblastoma [65]. In breast cancer, altered CHD7 levels correlate with aggressive disease behavior and inferior clinical outcomes [66]. Despite these associations, the contribution of CHD7 to therapeutic resistance and the precise pathways involved have not been fully elucidated. Aberrant activation of the PI3K/AKT and MAPK/ERK cascades is a hallmark of AML that is strongly linked to unfavorable prognosis and therapeutic resistance [67-69]. Our experiments show that CHD7 deletion activates both AKT and ERK signaling, which in turn reduces the responsiveness of AML cells to gilteritinib and venetoclax.

ANGPT1 belongs to the angiopoietin family and protects endothelial cells from apoptosis by stimulating the PI3K/AKT pathway upon binding to the TIE2 receptor [70, 71]. ANGPT1-TIE2 signaling additionally governs hematopoietic stem cell maturation [72]. High ANGPT1 expression is associated with poorer outcomes in both AML and myelodysplastic syndromes [73, 74]. Importantly, ANGPT1 engages TIE2 at distinct endothelial subcellular locations, eliciting spatially segregated signals: AKT is preferentially activated at cell-cell contacts, whereas ERK activation predominates at cell-matrix interfaces according to TIE2 distribution [49]. TIE2 activity is further fine-tuned through physical interactions with integrins α5β1 and αvβ3. These integrin partnerships heighten TIE2 sensitivity, particularly when extracellular matrix proteins such as fibronectin are present, leading to amplified ERK/MAPK signaling [75]. ANGPT1 also mediates paracrine communication; for instance, pericyte-derived extracellular vesicles carrying ANGPT1 can reinforce endothelial barrier properties and trigger PI3K/AKT activation in recipient cells, even during inflammation or cellular stress [76].

We report here the first demonstration that ANGPT1 is a direct downstream target negatively controlled by CHD7 in AML cells. Our data establish that ANGPT1 participates in the multidrug resistance phenotype driven by CHD7 loss. We further connect ANGPT1 function to the stimulation of AKT and ERK pathways, thereby strengthening the mechanistic understanding of CHD7's involvement in AML drug resistance. As a chromatin-remodeling protein, CHD7 occupies the ANGPT1 promoter and represses its transcription, most likely by preserving a compact chromatin configuration or by recruiting repressive chromatin-modifying complexes. In the absence of CHD7, chromatin accessibility at the ANGPT1 promoter increases, resulting in elevated ANGPT1 transcription. These molecular findings are consistent with the observed cellular phenotypes and uncover an epigenetic regulatory circuit in which CHD7 restrains ANGPT1 expression and the consequent activation of AKT and ERK, thereby modulating drug sensitivity in AML. Based on these insights, we propose pharmacological disruption of the ANGPT1-TIE2 pathway as a strategy to reverse resistance to gilteritinib and venetoclax in CHD7-deficient

AML. Experimental testing confirmed synergistic interactions between TIE2 inhibitors and either gilteritinib or venetoclax in AML cell models.

Overall, this work uncovers a previously unrecognized drug-resistance mechanism in AML orchestrated by the CHD7-ANGPT1 axis. In contrast to classical resistance routes centered on direct genetic modification of drug targets (e.g., FLT3 mutations) or engagement of standard anti-apoptotic pathways (such as BCL2 overexpression), CHD7 operates as an epigenetic regulator that elevates ANGPT1 levels, activates TIE2-dependent signaling, and sustains leukemic cell viability. This interplay between chromatin remodeling and extrinsic microenvironmental cues defines a non-canonical resistance program [77] Clinically, multiple TIE2 inhibitors (e.g., rebastinib) and ANGPT1/2-neutralizing antibodies (e.g., nesvacumab) have already shown manageable safety profiles in early clinical studies for other tumor types [78, 79]. Although not yet approved for AML, these agents represent attractive candidates for therapeutic repurposing. Importantly, we validated the translational relevance of TIE2 blockade by demonstrating strong synergy with frontline AML drugs, including gilteritinib and venetoclax, in primary patient AML specimens. Such combinations substantially augment anti-leukemic potency and supply solid preclinical justification for advancing TIE2-directed therapies into clinical testing for AML.

In brief, our findings establish CHD7 as a central player in multidrug resistance in AML. We also show that CHD7 loss markedly impairs apoptosis while enhancing AML cell proliferation in both cell culture and animal models. Finally, identification of the CHD7-ANGPT1 regulatory axis reveals several actionable nodes for therapeutic intervention in this disease.

Conclusion

In summary, a CRISPR-Cas9 knockout screen enabled the discovery of CHD7 as a novel controller of drug resistance in AML. Subsequent functional studies confirmed that CHD7 inactivation confers resistance to several key AML therapies, with pronounced effects on gilteritinib and venetoclax. Comprehensive multi-omics integration of transcriptomic and proteomic data demonstrated that CHD7 deficiency drives robust upregulation of ANGPT1, leading to activation of the downstream PI3K/AKT and MAPK/ERK cascades. Preclinical evaluation further revealed that targeted inhibition of the ANGPT1-TIE2 pathway can resensitize CHD7-deficient AML cells to these drugs. Collectively, these results deepen our understanding of the molecular underpinnings of therapeutic resistance in AML and position the CHD7-ANGPT1 axis as a viable target for intervention. Pairing TIE2 inhibitors with established AML agents emerges as a promising therapeutic avenue to surmount resistance and enhance patient prognosis. Future clinical studies will be essential to corroborate these observations and to optimize additional combination regimens.

Acknowledgments: None

Conflict of Interest: None

Financial Support: None

Ethics Statement: None

References

1. Döhner H, Weisdorf DJ, Bloomfield CD. Acute myeloid leukemia. N Engl J Med. 2015;373(12):1136-52. doi:10.1056/NEJMra1406184
2. Papaemmanuil E, Gerstung M, Bullinger L, Gaidzik VI, Paschka P, Roberts ND, et al. Genomic classification and prognosis in acute myeloid leukemia. N Engl J Med. 2016;374(23):2209-21. doi:10.1056/NEJMoa1516192
3. Yi M, Li A, Zhou L, Chu Q, Song Y, Wu K. The global burden and attributable risk factor analysis of acute myeloid leukemia in 195 countries and territories from 1990 to 2017: estimates based on the Global Burden of Disease Study 2017. J Hematol Oncol. 2020;13:72. doi:10.1186/s13045-020-00908-z
4. Zou Y, Zhang H, Hu H. Big data and single-cell sequencing in acute myeloid leukemia research. MedComm (Oncol). 2023;2:e47. doi:10.1002/mog2.47

5. Ferrara F, Schiffer CA. Acute myeloid leukaemia in adults. Lancet. 2013;381(9865):484-95. doi:10.1016/S0140-6736(12)61727-9
6. Liu H. Emerging agents and regimens for AML. J Hematol Oncol. 2021;14(1):49. doi:10.1186/s13045-021-01062-w
7. Levis M, Small D. FLT3: ITDoes matter in leukemia. Leukemia. 2003;17(9):1738-52. doi:10.1038/sj.leu.2403099
8. Grob T, Sanders MA, Vonk CM, Kavelaars FG, Rijken M, Hanekamp DW, et al. Prognostic value of FLT3-internal tandem duplication residual disease in acute myeloid leukemia. J Clin Oncol. 2023;41(4):756-65. doi:10.1200/JCO.22.00715
9. Daver N, Schlenk RF, Russell NH, Levis MJ. Targeting FLT3 mutations in AML: review of current knowledge and evidence. Leukemia. 2019;33(2):299-312. doi:10.1038/s41375-018-0357-9
10. McMahon CM, Ferng T, Canaani J, Wang ES, Morrissette JJD, Eastburn DJ, et al. Clonal selection with RAS pathway activation mediates secondary clinical resistance to selective FLT3 inhibition in acute myeloid leukemia. Cancer Discov. 2019;9(8):1050-65. doi:10.1158/2159-8290.CD-18-1452
11. Levis M, Perl AE. Gilteritinib: potent targeting of FLT3 mutations in AML. Blood Adv. 2020;4(6):1178-91. doi:10.1182/bloodadvances.2019000174
12. Kayser S, Levis MJ. Updates on targeted therapies for acute myeloid leukaemia. Br J Haematol. 2022;196(2):316-28. doi:10.1111/bjh.17746
13. Perl AE, Martinelli G, Cortes JE, Neubauer A, Berman E, Paolini S, et al. Gilteritinib or chemotherapy for relapsed or refractory FLT3-mutated AML. N Engl J Med. 2019;381(18):1728-40. doi:10.1056/NEJMoa1902688
14. Zhao JC, Agarwal S, Ahmad H, Amin K, Bewersdorf JP, Zeidan AM. A review of FLT3 inhibitors in acute myeloid leukemia. Blood Rev. 2022;52:100905. doi:10.1016/j.blre.2021.100905
15. Pei S, Pollyea DA, Gustafson A, Stevens BM, Minhajuddin M, Fu R, et al. Monocytic subclones confer resistance to venetoclax-based therapy in patients with acute myeloid leukemia. Cancer Discov. 2020;10(4):536-51. doi:10.1158/2159-8290.CD-19-0710
16. Vasu S, Kohlschmidt J, Mrózek K, Eisfeld AK, Nicolet D, Sterling LJ, et al. Ten-year outcome of patients with acute myeloid leukemia not treated with allogeneic transplantation in first complete remission. Blood Adv. 2018;2(13):1645-50. doi:10.1182/bloodadvances.2017015222
17. Sasaki K, Ravandi F, Kadia TM, DiNardo CD, Short NJ, Borthakur G, et al. De novo acute myeloid leukemia: a population-based study of outcome in the United States based on the Surveillance, Epidemiology, and End Results (SEER) database, 1980 to 2017. Cancer. 2021;127(12):2049-61. doi:10.1002/cncr.33458
18. Joshi SK, Nechiporuk T, Bottomly D, Piehowski PD, Reisz JA, Pittsenbarger J, et al. The AML microenvironment catalyzes a stepwise evolution to gilteritinib resistance. Cancer Cell. 2021;39(7):999-1014.e8. doi:10.1016/j.ccell.2021.06.003
19. Eguchi M, Minami Y, Kuzume A, Chi S. Mechanisms underlying resistance to FLT3 inhibitors in acute myeloid leukemia. Biomedicines. 2020;8(8):245. doi:10.3390/biomedicines8080245
20. Ruglioni M, Crucitta S, Luculli GI, Tancredi G, Del Giudice ML, Mechelli S, et al. Understanding mechanisms of resistance to FLT3 inhibitors in adult FLT3-mutated acute myeloid leukemia to guide treatment strategy. Crit Rev Oncol Hematol. 2024;201:104424. doi:10.1016/j.critrevonc.2024.104424
21. Garciaz S, Hospital MA, Collette Y, Vey N. Venetoclax resistance in acute myeloid leukemia. Cancers (Basel). 2024;16(6):1091. doi:10.3390/cancers16061091
22. Sullivan GP, Flanagan L, Rodrigues DA, Ní Chonghaile T. The path to venetoclax resistance is paved with mutations, metabolism, and more. Sci Transl Med. 2022;14(674):eabo6891. doi:10.1126/scitranslmed.abo6891
23. Zhang Q, Riley-Gillis B, Han L, Jia Y, Lodi A, Zhang H, et al. Activation of RAS/MAPK pathway confers MCL-1 mediated acquired resistance to BCL-2 inhibitor venetoclax in acute myeloid leukemia. Signal Transduct Target Ther. 2022;7(1):51. doi:10.1038/s41392-021-00870-3
24. Hsu J, Huang HT, Lee CT, Choudhuri A, Wilson NK, Abraham BJ, et al. CHD7 and Runx1 interaction provides a braking mechanism for hematopoietic differentiation. Proc Natl Acad Sci U S A. 2020;117(38):23626-35. doi:10.1073/pnas.2003228117
25. Kissa K, Herbomel P. Blood stem cells emerge from aortic endothelium by a novel type of cell transition. Nature. 2010;464(7285):112-5. doi:10.1038/nature08761

26. Yzaguirre AD, Howell ED, Li Y, Liu Z, Speck NA. Runx1 is sufficient for blood cell formation from non-hemogenic endothelial cells in vivo only during early embryogenesis. Development. 2018;145(2):dev158162. doi:10.1242/dev.158162
27. Canu G, Ruhrberg C. First blood: the endothelial origins of hematopoietic progenitors. Angiogenesis. 2021;24(2):199-211. doi:10.1007/s10456-021-09783-9
28. Zhen T, Kwon EM, Zhao L, Hsu J, Hyde RK, Lu Y, et al. Chd7 deficiency delays leukemogenesis in mice induced by Cbfb-MYH11. Blood. 2017;130(22):2431-42. doi:10.1182/blood-2017-04-780106
29. Tao Y, Zhang Q, Long S, Li X, Chen J, Li X. Shifts of lipid metabolites help decode immobilization of soil cadmium under reductive soil disinfestation. Sci Total Environ. 2022;829:154592. doi:10.1016/j.scitotenv.2022.154592
30. Lu M, Ding N, Zhuang S, Li Y. LINC01410/miR-23c/CHD7 functions as a ceRNA network to affect the prognosis of patients with endometrial cancer and strengthen the malignant properties of endometrial cancer cells. Mol Cell Biochem. 2020;469(1-2):9-19. doi:10.1007/s11010-020-03723-9
31. Colbert LE, Petrova AV, Fisher SB, Pantazides BG, Madden MZ, Hardy CW, et al. CHD7 expression predicts survival outcomes in patients with resected pancreatic cancer. Cancer Res. 2014;74(10):2677-87. doi:10.1158/0008-5472.CAN-13-1996
32. Zhang Z, Huang D, Feng J, Li W, Wang Z, Lu M, et al. PDE5 inhibitors against cancer via mediating immune cells in tumor microenvironment: AI-based approach for future drug repurposing exploration. Interdiscip Med. 2024;2:e20230062. doi:10.1002/INMD.20230062
33. Kim KY, Kim BJ, Yi GS. Reuse of imputed data in microarray analysis increases imputation efficiency. BMC Bioinformatics. 2004;5:160
34. Wang S, Li W, Hu L, Cheng J, Yang H, Liu Y. NAguideR: performing and prioritizing missing value imputations for consistent bottom-up proteomic analyses. Nucleic Acids Res. 2020;48(14):e83. doi:10.1093/nar/gkaa498
35. McMahon CM, Perl AE. Gilteritinib for the treatment of relapsed and/or refractory FLT3-mutated acute myeloid leukemia. Expert Rev Clin Pharmacol. 2019;12(9):841-9. doi:10.1080/17512433.2019.1657009
36. Shimada K, Bachman JA, Muhlich JL, Mitchison TJ. shinyDepMap, a tool to identify targetable cancer genes and their functional connections from Cancer Dependency Map data. eLife. 2021;10:e57116. doi:10.7554/eLife.57116
37. Li W, Xu H, Xiao T, Cong L, Love MI, Zhang F, et al. MAGeCK enables robust identification of essential genes from genome-scale CRISPR/Cas9 knockout screens. Genome Biol. 2014;15(12):554. doi:10.1186/s13059-014-0554-4
38. Honda A, Koya J, Yoshimi A, Miyauchi M, Taoka K, Kataoka K, et al. Loss-of-function mutations in BCOR contribute to chemotherapy resistance in acute myeloid leukemia. Exp Hematol. 2021;101-102:42-8.e11. doi:10.1016/j.exphem.2021.07.005
39. Lin X, Chen H, Xie Y, Zhou X, Wang Y, Zhou J, et al. Combination of CTLA-4 blockade with MUC1 mRNA nanovaccine induces enhanced anti-tumor CTL activity by modulating tumor microenvironment of triple negative breast cancer. Transl Oncol. 2022;15(1):101298. doi:10.1016/j.tranon.2021.101298
40. Zhang Z, Zhou C, Li X, Barnes SD, Deng S, Hoover E, et al. Loss of CHD1 promotes heterogeneous mechanisms of resistance to AR-targeted therapy via chromatin dysregulation. Cancer Cell. 2020;37(4):584-98.e11. doi:10.1016/j.ccell.2020.03.001
41. Galanis A, Ma H, Rajkhowa T, Ramachandran A, Small D, Cortes J, et al. Crenolanib is a potent inhibitor of FLT3 with activity against resistance-conferring point mutants. Blood. 2014;123(1):94-100. doi:10.1182/blood-2013-10-529313
42. Zarrinkar PP, Gunawardane RN, Cramer MD, Gardner MF, Brigham D, Belli B, et al. AC220 is a uniquely potent and selective inhibitor of FLT3 for the treatment of acute myeloid leukemia (AML). Blood. 2009;114(14):2984-92. doi:10.1182/blood-2009-05-222034
43. DiNardo CD, Pratz K, Pullarkat V, Jonas BA, Arellano M, Becker PS, et al. Venetoclax combined with decitabine or azacitidine in treatment-naive, elderly patients with acute myeloid leukemia. Blood. 2019;133(1):7-17. doi:10.1182/blood-2018-08-868752
44. Pollyea DA, Pratz K, Letai A, Jonas BA, Wei AH, Pullarkat V, et al. Outcomes in patients with poor-risk features after frontline venetoclax combined with azacitidine or decitabine for acute myeloid leukemia. Am J Hematol. 2021;96:208-17. doi:10.1002/ajh.26017

45. DiNardo CD, Pratz KW, Letai A, Jonas BA, Wei AH, Thirman M, et al. Safety and preliminary efficacy of venetoclax with decitabine or azacitidine in elderly patients with previously untreated acute myeloid leukaemia: A non-randomised, open-label, phase 1b study. Lancet Oncol. 2018;19(2):216-28. doi:10.1016/S1470-2045(18)30010-X
46. Blair HA. Daunorubicin/cytarabine liposome: A review in acute myeloid leukaemia. Drugs. 2018;78(18):1903-10. doi:10.1007/s40265-018-1022-3
47. Pollyea DA. Therapeutic advances in first-line management of acute myeloid leukemia. J Natl Compr Canc Netw. 2019;17(11.5):1441-3. doi:10.6004/jnccn.2019.5031
48. Fukuhara S, Sako K, Noda K, Nagao K, Miura K, Mochizuki N. Tie2 is tied at the cell-cell contacts and to extracellular matrix by Angiopoietin-1. Exp Mol Med. 2009;41:133-9. doi:10.3858/emm.2009.41.3.015
49. Fukuhara S, Sako K, Minami T, Noda K, Kim HZ, Kodama T, et al. Differential function of Tie2 at cell-cell contacts and cell-substratum contacts regulated by angiopoietin-1. Nat Cell Biol. 2008;10(5):513-26. doi:10.1038/ncb1714
50. Hsieh FK, Ji F, Damle M, Sadreyev RI, Kingston RE. HERVH-derived lncRNAs negatively regulate chromatin targeting and remodeling mediated by CHD7. Life Sci Alliance. 2022;5(1):e202101127. doi:10.26508/lsa.202101127
51. Chai M, Sanosaka T, Okuno H, Zhou Z, Koya I, Banno S, et al. Chromatin remodeler CHD7 regulates the stem cell identity of human neural progenitors. Genes Dev. 2018;32(2):165-80. doi:10.1101/gad.301887.117
52. Sethi A, Gu M, Gumusgoz E, Chan L, Yan KK, Rozowsky J, et al. Supervised enhancer prediction with epigenetic pattern recognition and targeted validation. Nat Methods. 2020;17:807-14.
53. Semones M, Feng Y, Johnson N, Adams JL, Winkler J, Hansbury M. Pyridinylimidazole inhibitors of Tie2 kinase. Bioorg Med Chem Lett. 2007;17(17):4756-60. doi:10.1016/j.bmcl.2007.06.068
54. Bhansali RS, Pratz KW, Lai C. Recent advances in targeted therapies in acute myeloid leukemia. J Hematol Oncol. 2023;16(1):29. doi:10.1186/s13045-023-01424-6
55. Thol F, Döhner H, Ganser A. How I treat refractory and relapsed acute myeloid leukemia. Blood. 2024;143(1):11-20. doi:10.1182/blood.2023022481
56. Peroni E, Randi ML, Rosato A, Cagnin S. Acute myeloid leukemia: From NGS, through scRNA-seq, to CAR-T. Dissect cancer heterogeneity and tailor the treatment. J Exp Clin Cancer Res. 2023;42(1):259. doi:10.1186/s13046-023-02841-8
57. Tzelepis K, Koike-Yusa H, De Braekeleer E, Li Y, Metzakopian E, Dovey OM, et al. A CRISPR dropout screen identifies genetic vulnerabilities and therapeutic targets in acute myeloid leukemia. Cell Rep. 2016;17(4):1193-205. doi:10.1016/j.celrep.2016.09.079
58. Basheer FT, Vassiliou GS. Genome-scale drop-out screens to identify cancer cell vulnerabilities in AML. Curr Opin Genet Dev. 2019;54:83-7. doi:10.1016/j.gde.2019.04.004
59. Jaiswal AK, Truong H, Tran TM, Lin TL, Casero D, Alberti MO, et al. Focused CRISPR-Cas9 genetic screening reveals USO1 as a vulnerability in B-cell acute lymphoblastic leukemia. Sci Rep. 2021;11:13158. doi:10.1038/s41598-021-92448-w
60. Wang Y, Ma X, Zhang T, Wang L, Liu Y, Zhou G, et al. Research progress of DNA methylation in the screening of cervical cancer and precancerous lesions. Interdiscip Med. 2025;3:e20240043. doi:10.1002/INMD.20240043
61. Schnetz MP, Handoko L, Akhtar-Zaidi B, Bartels CF, Pereira CF, Fisher AG, et al. CHD7 targets active gene enhancer elements to modulate ES cell-specific gene expression. PLoS Genet. 2010;6(7):e1001023. doi:10.1371/journal.pgen.1001023
62. Gao J, Skidmore JM, Cimerman J, Ritter KE, Qiu J, Wilson LMQ, et al. CHD7 and SOX2 act in a common gene regulatory network during mammalian semicircular canal and cochlear development. Proc Natl Acad Sci U S A. 2024;121(10):e2311720121. doi:10.1073/pnas.2311720121
63. Rother MB, Pellegrino S, Smith R, Gatti M, Meisenberg C, Wiegant WW, et al. CHD7 and 53BP1 regulate distinct pathways for the re-ligation of DNA double-strand breaks. Nat Commun. 2020;11:5775. doi:10.1038/s41467-020-19502-5
64. Vissers LELM, van Ravenswaaij CMA, Admiraal R, Hurst JA, de Vries BBA, Janssen IM, et al. Mutations in a new member of the chromodomain gene family cause CHARGE syndrome. Nat Genet. 2004;36(9):955-7. doi:10.1038/ng1407

65. Badodi S, Dubuc A, Zhang X, Rosser G, Da Cunha Jaeger M, Kameda-Smith MM, et al. Convergence of BMI1 and CHD7 on ERK signaling in medulloblastoma. Cell Rep. 2017;21(10):2772-84. doi:10.1016/j.celrep.2017.11.021
66. Chu X, Guo X, Jiang Y, Yu H, Liu L, Shan W, et al. Genotranscriptomic meta-analysis of the CHD family chromatin remodelers in human cancers: initial evidence of an oncogenic role for CHD7. Mol Oncol. 2017;11(10):1348-60. doi:10.1002/1878-0261.12104
67. Darici S, Alkhaldi H, Horne G, Jørgensen HG, Marmiroli S, Huang X. Targeting PI3K/Akt/mTOR in AML: rationale and clinical evidence. J Clin Med. 2020;9(9):2934. doi:10.3390/jcm9092934
68. Nepstad I, Hatfield KJ, Grønningsæter IS, Reikvam H. The PI3K-Akt-mTOR signaling pathway in human acute myeloid leukemia (AML) cells. Int J Mol Sci. 2020;21(8):2907. doi:10.3390/ijms21082907
69. Park S, Chapuis N, Tamburini J, Bardet V, Cornillet-Lefebvre P, Willems L, et al. Role of the PI3K/AKT and mTOR signaling pathways in acute myeloid leukemia. Haematologica. 2010;95(5):819-28. doi:10.3324/haematol.2009.013797
70. Li AQ, Fang JH. Anti-angiogenic therapy enhances cancer immunotherapy: mechanism and clinical application. Interdiscip Med. 2024;2:e20230025. doi:10.1002/INMD.20230025
71. Stephen NM, Deepika UR, Maradagi T, Sugawara T, Hirata T, Ganesan P. Insight on the cellular and molecular basis of blood vessel formation: A specific focus on tumor targets and therapy. MedComm Oncol. 2023;2:e22. doi:10.1002/mog2.22
72. Ikushima YM, Arai F, Nakamura Y, Hosokawa K, Kubota Y, Hirashima M, et al. Enhanced Angpt1/Tie2 signaling affects the differentiation and long-term repopulation ability of hematopoietic stem cells. Biochem Biophys Res Commun. 2013;430(1):20-5. doi:10.1016/j.bbrc.2012.11.002
73. Bachegowda L, Morrone K, Winski SL, Mantzaris I, Bartenstein M, Ramachandra N, et al. Pexmetinib: a novel dual inhibitor of Tie2 and p38 MAPK with efficacy in preclinical models of myelodysplastic syndromes and acute myeloid leukemia. Cancer Res. 2016;76(16):4841-9. doi:10.1158/0008-5472.CAN-15-3062
74. Ma D, Liu P, Hu C, Zhou Z, Wang P, Wang Y, et al. Intracellular angiopoietin-1 promotes TKI-resistance via activation of JAK/STAT5 pathway in chronic myeloid leukemia. Oncogene. 2023;42(2):124-37. doi:10.1038/s41388-022-02536-y
75. Dalton AC, Shlamkovitch T, Papo N, Barton WA. Constitutive association of Tie1 and Tie2 with endothelial integrins is functionally modulated by angiopoietin-1 and fibronectin. PLoS One. 2016;11(10):e0163732. doi:10.1371/journal.pone.0163732
76. Zhang ZS, Yang A, Luo X, Zhou HN, Liu YY, Bao DQ, et al. Pericyte-derived extracellular vesicles improve vascular barrier function in sepsis via the Angpt1/PI3K/AKT pathway and pericyte recruitment: an in vivo and in vitro study. Stem Cell Res Ther. 2025;16(1):70. doi:10.1186/s13287-025-04201-z
77. Huang H, Bhat A, Woodnutt G, Lappe R. Targeting the ANGPT-TIE2 pathway in malignancy. Nat Rev Cancer. 2010;10(8):575-85. doi:10.1038/nrc2894
78. Anampa JD, Flynn DL, Leary C, Oh S, Xue X, Oktay MH, et al. Phase Ib clinical and pharmacodynamic study of the TIE2 kinase inhibitor rebastinib with paclitaxel or eribulin in HER2-negative metastatic breast cancer. Clin Cancer Res. 2025;31(2):266-77. doi:10.1158/1078-0432.CCR-24-2464
79. Papadopoulos KP, Kelley RK, Tolcher AW, Abdul Razak AR, Van Loon K, Patnaik A, et al. A phase I first-in-human study of nesvacumab (REGN910), a fully human anti-angiopoietin-2 (Ang2) monoclonal antibody, in patients with advanced solid tumors. Clin Cancer Res. 2016;22(6):1348-55. doi:10.1158/1078-0432.CCR-15-1221